Graphene Quantum Dots-Band-Aids Used for Wound Disinfection

Hanjun Sun, Nan Gao, Kai Dong, Jinsong Ren, and Xiaogang Qu*

Laboratory of Chemical Biology, Division of Biological Inorganic Chemistry, State Key Laboratory of Rare Earth Resource Utilization, Changchun Institute of Applied Chemistry, University of Chinese Academy of Sciences, Changchun, Jilin 130022, China

ABSTRACT Herein, an antibacterial system combining the "safe" carbon nanomaterials, graphene quantum dots (GQDs), with a low level of H_2O_2 has been put forward. It has been found that the peroxidase-like activity of GQDs originates from their ability to catalyze the decomposition of H_2O_2, generating ·OH. Since the ·OH has a higher antibacterial activity, the conversion of H_2O_2 into ·OH improves the antibacterial performance of H_2O_2, which makes it possible to avoid the toxicity of H_2O_2 at high levels in wound disinfection. All the experiments *in vitro* display that this intrinsic activity exerts a high enhancement of antibacterial activity of H_2O_2, and the designed system possessed broad spectrum of antibacterial activity against both Gram-negative (*Escherichia coli*) and Gram-positive (*Staphylococcus aureus*) bacteria. More importantly, to assess the antibacterial efficacy of the designed system in actual wound disinfection, the GQD-Band-Aids are prepared and show excellent antibacterial property with the assistance of H_2O_2 at low dose *in vivo*.

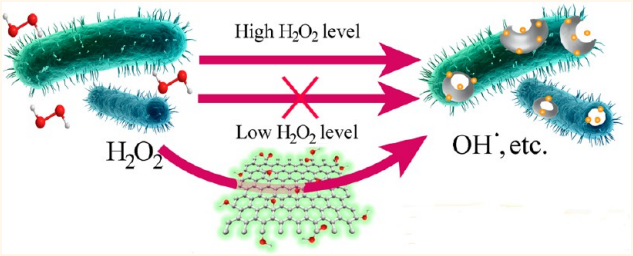

KEYWORDS: graphene quantum dots · peroxidase-like activity · antibacterial system · Band-Aid · wound disfenction

Infectious diseases induced by bacteria continue to be one of the greatest health problems worldwide, afflicting millions of people annually.[1] Antibacterial materials are widely used in daily life and effectively protect the public health.[1] A series of drugs or materials, including antibiotics,[2] metal ions,[3] and quaternary ammonium compounds,[4] can inhibit bacteria growth and destroy cellular structure of microorganisms. However, it is known that the above materials are associated with concerns about antibiotic resistance, environmental pollution, complex chemical synthesis, and high cost.[2−4] More recently, antibacterial nanomaterials, including nanosilver, nanometal oxide, carbon nanotubes (CNTs), graphene, *etc.*, have been explored to overcome these disadvantages.[1,5−11] Among these antibacterial nanomaterials, carbon nanomaterials are renewable, easier to obtain and cheaper than Ag and metal oxide.[8] Unfortunately, CNTs, which can easily pierce cells, have been reported to be cytotoxic for both human cells and bacteria.[6] Graphene and its drivatives have high antibacterial activity due to physical damages occurred upon direct contact to bacterial membranes by sharp edges of graphene sheets; however, the improved oxidative stress induced by graphene-based material can lead to the apoptosis of mammalian cells.[12] Thus, the exploration of biocompatible carbon nanomaterials is necessary in this field.

Graphene quantum dots (GQDs), as defined, are a kind of 0D material with characteristics derived from both graphene and carbon dots (CDs), which can be regarded as very tiny pieces of graphene.[13−17] Compared with organic dyes and semiconductive quantum dots (QDs), GQDs are superior in terms of their excellent properties, such as high photostability against photobleaching and blinking. Unlike their cousins, CDs, GQDs clearly possess graphene's structure inside the dots regardless of the dot size, which endows them with some unordinary properties of graphene.[13−17] More importantly, GQDs have been found to have lower toxicity than graphene oxide (GO)[18] and cause no apparent toxicity *in vivo*.[19] For these reasons, the GQDs have attracted great attention in materials science and biological applications.[13−17] Especially in the area of biomedicine, significant progress has been achieved for the utilization

* Address correspondence to xqu@ciac.ac.cn.

Received for review March 25, 2014 and accepted May 28, 2014.

Published online May 28, 2014
10.1021/nn501640q

of GQDs in cellular imaging, biosensors and drug delivery.[13−17]

In addition, GQDs possess higher peroxidase-like activity than graphene due to their excellent electron transportation property.[17,20−22] Up to now, the study of peroxidase-like activity of GQDs is mainly focused on biosensing,[17,20−22] and its pharmacological activity in antibacterial field has not been reported. As a medical reagent, H_2O_2 is widely used in wound disinfection to avoid bacterial infection. Nevertheless, the antibacterial activity of H_2O_2 is lower than hydroxyl radical (·OH),[23] and the concentration of H_2O_2 used in disinfection is high (usually 0.5−3%, *ca.* 166 mM to 1 M).[24−26] The high concentration of H_2O_2 is also harmful to healthy tissue[27,28] and even delays wound healing.[26] Consequently, improving the antibacterial activity of H_2O_2 and lowering the "high concentration" used for efficacious germicidal efficacy are demanding for wound disinfection. Recently, functional inorganic analogues, such as V_2O_5 and magnetic iron oxide, have been used to assist H_2O_2 for antibacterial application.[29,30] Tremel and co-workers have demonstrated that V_2O_5 nanowires with vanadium haloperoxidases-like activity can produce HOBr and $^1O_2$ species. This intrinsic activity displays a strong antibacterial activity against both Gram-negative (*Escherichia coli*) and Gram-positive (*Staphylococcus aureus*) bacteria.[29] Very recently, Gao *et al.* have reported ferromagnetic nanoparticles with peroxidase-like activity can enhance oxidative cleavage of bacterial biofilm components in the presence of H_2O_2 at the concentration of 1%, breaking down the existing biofilm and preventing formation of new biofilm.[30] However, the V_2O_5 and magnetic iron oxide were considered to be toxic and inappropriate for the application *in vivo* unless *via* elaborate surface functionalization.[31−34] Herein, taking the advantages of both peroxidase-like activity and excellent biocompatibility of GQDs, an antibacterial system based on GQDs and low dose of H_2O_2 has been designed (Scheme 1A). The presence of GQDs can convert H_2O_2 (low antibacterial activity) into ·OH radicals (high antibacterial activity), thus improving the antibacterial performance of H_2O_2, which makes it possible to avoid using high concentration of H_2O_2 in wound disinfection. The designed system possessed broad spectrum of antibacterial activity against both Gram-negative (*E. coli*) and Gram-positive (*S. aureus*) bacteria. What's more, the GQD-Band-Aids were prepared and used in wound disinfection *in vivo* (Scheme 1B).

RESULTS AND DISCUSSION

The green luminescent GQDs were synthesized according to previous reports.[35−37] The characterizations of the as-prepared GQDs were shown in Figure 1 and Figure S1 (Supporting Information). The typical transmission electron microscope (TEM) images and

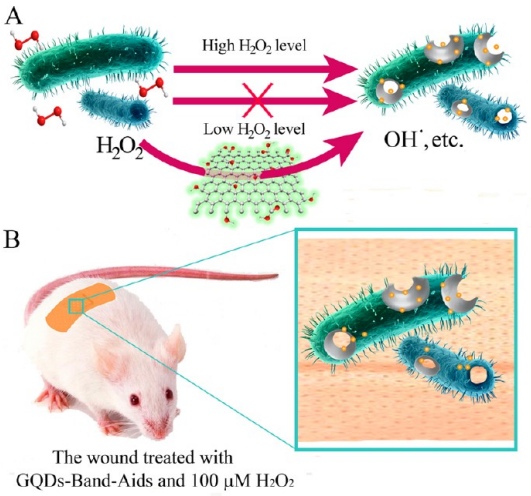

Scheme 1. (A) The designed system based on GQDs and low level of H_2O_2 for the antibacterial application. (B) The GQD-Band-Aids used in wound disinfection *in vivo*.

atomic force microscopy (AFM) images showed that GQDs were well dispersed (Figure 1A,C). For GQDs, the size distributions (3−8 nm), height distributions (0.4−2 nm), the average size (5.1 nm) and average height (1.3 nm) were similar to the literatures (Figure 1D,E). Furthermore, high-resolution TEM (HRTEM) images showed GQDs had crystallinity with lattice of 0.21 nm (Figure 1B), which was consistent with the (102) diffraction planes of sp^2 graphitic carbon, implying that GQDs kept the similar crystallinity with graphene.[35−37] In addition, the results of UV−vis absorption, photoluminescence (PL) spectroscopy, Fourier transform infrared (FT-IR) spectroscopy and X-ray photoelectron spectroscopy (XPS) were consistent with those previously reported (Figure S1, Supporting Information).[35−37] The peroxidase-like activity of the GQDs was evaluated by catalytic oxidation of 2,2′-azinobis(3-ethylbenzthiazoline-6-sulfonate) (ABTS) in the presence of H_2O_2. As shown in Figure S2A−D (Supporting Information), the catalytic activity of GQDs was dependent on pH, temperature and concentration, which was similar to those of natural peroxidase and graphene oxide.[20−22,38] Under our experimental conditions, the optimal pH and temperature were pH 4.0 and 37 °C. Moreover, in a certain range of H_2O_2 concentrations, typical Michaelis−Menten curves could be obtained for GQDs and GO. Maximum initial velocity (V_{max}) and Michaelis−Menten constant (K_m) were estimated by using Lineweaver−Burk plot (Figure S2E, Supporting Information), and the results were summarized in Table S1 (Supporting Information). The GQDs showed higher peroxidase-like activity than graphene oxide (GO), which might be contributed to its better electron transportation property.[17,20] Even the optimal pH of GQDs was pH 4.0; they still displayed certain peroxidase-like activity at pH 7.4, which promised their usage in biologic field (Figure S2F, Supporting Information).

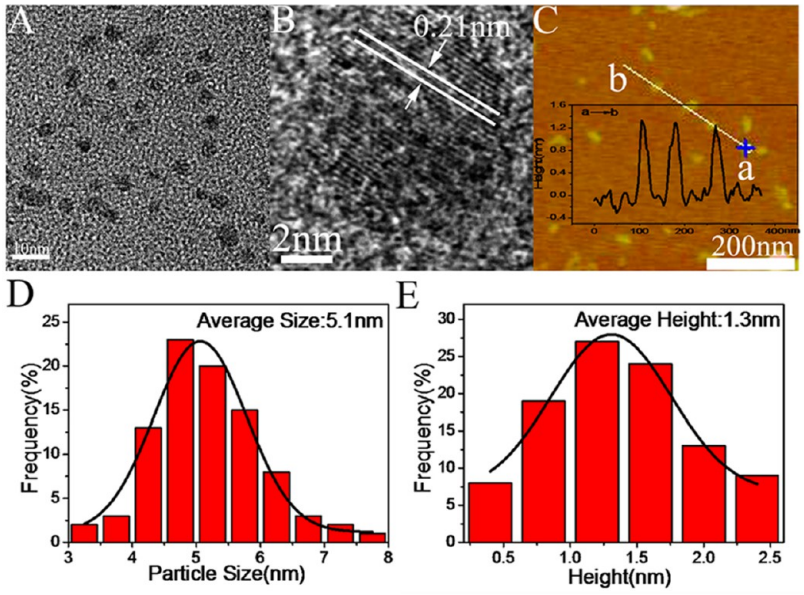

Figure 1. (A) TEM images of GQDs. (B) Representative images of individual GQDs. (C) The AFM images of GQDs. Insets of C are corresponding height profile of GQDs. (D,E) Particle size distributions and height distributions of GQDs.

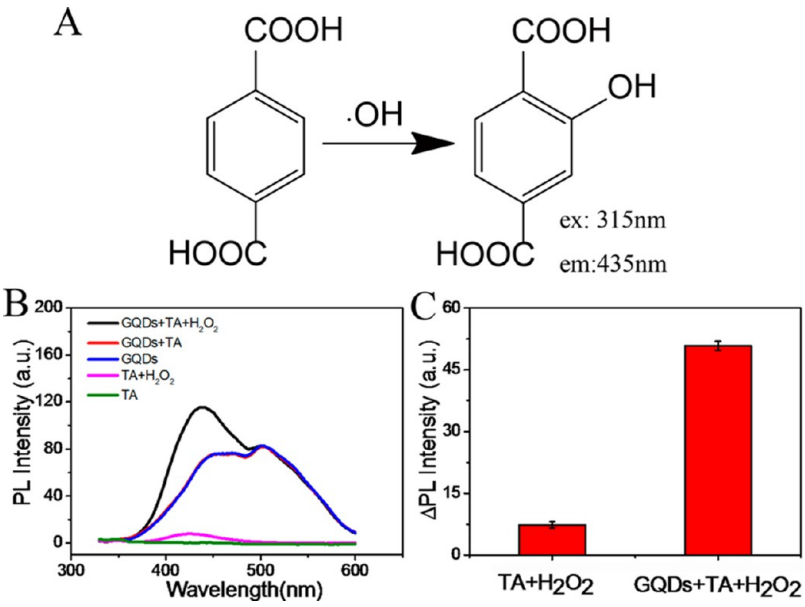

Figure 2. (A) Reaction between hydroxyl radical (·OH) and terephthalic acid (TA). (B) Fluorescence spectra of the PBS solution (pH = 7.4, 25 mM) include only TA; TA and H_2O_2; only GQDs; TA and GQDs; TA, GQDs and H_2O_2 after 12 h reaction. The concentrations of TA, H_2O_2 and GQDs were 0.5 mM, 1 mM and 100 μg/mL, respectively. (C) Histograms of ΔPL intensity showed the catalysis effect of GQDs; error bars were taken from three parallel experiments.

Unlike other nanoenzymes, such as Fe_3O_4, Co_3O_4, CeO_2, *etc.*, the mechanism of GQDs' peroxidase-like activity had not been well understood.[17,20−22] Considering that the peroxidase-like activity of most nanoenzymes may originate from their catalytic ability toward the decomposition of H_2O_2 to generate hydroxyl radical (·OH),[39] fluorescence and chemiluminescence (CL) experiments were carried out to detect ·OH during the reaction. Terephthalic acid (TA) was used as a fluorescence probe for tracking of ·OH because it could capture ·OH and generate 2-hydroxy terephthalic acid (TAOH), which emitted unique fluorescence around 435 nm (Figure 2A).[40,41] Figure 2B,C showed the fluorescence change in the mixed solution of GQDs, TA and H_2O_2. After 12 h reaction, compared with control experiments, remarkable fluorescence enhancement at 435 nm indicated the presence of ·OH radicals.[41] CL experiments showed after the addition of GQDs, the hydroxyl radical scavenger, mannitol, was much more effective as an inhibitor of luminol's CL than the singlet oxygen scavenger, sodium azide (Figure S3, Supporting Information). Similar to fluorescence experiments, the

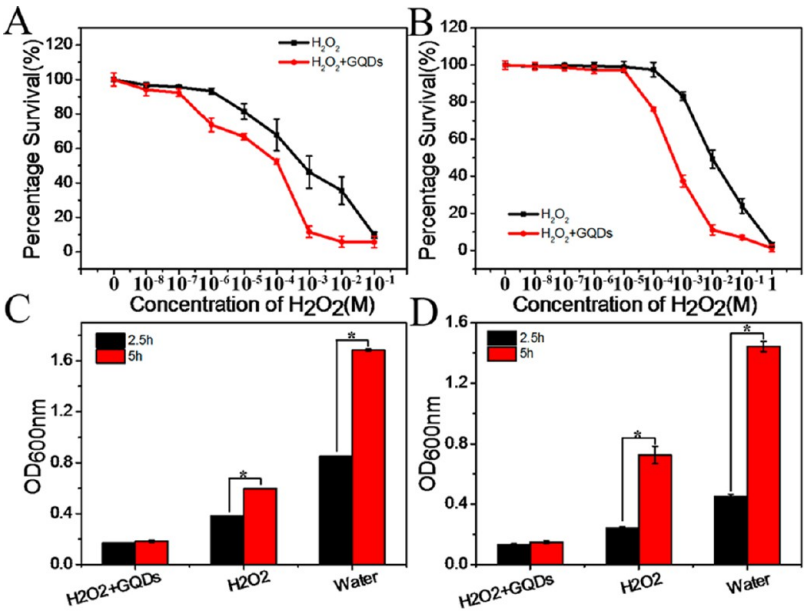

Figure 3. Survival rates of *E. coli* (A) and *S. aureus* (B) treated with H_2O_2 at different concentration coincubation with or without GQDs (100 μg/mL). Optical density at 600 nm (OD_{600nm}) of bacterial suspension treated with 100 μg/mL GQDs and 1 mM H_2O_2 (*E. coli*) (C) and 10 mM H_2O_2 (*S. aureus*) (D) at 2.5 and 5 h. The original bacterial concentration is 1×10^6 cfu mL^{-1}. *Significantly different ($P < 0.05$) from data obtained. There were no significant differences between the ODs at 2.5 and 5 h of *E. coli* and *S. aureus* after treatment with both GQDs and H_2O_2, which indicated the enhanced antibacterial activity of H_2O_2 by GQDs could also inhibit the growth of both *E. coli* and *S. aureus* bacteria.

strong quenching of CL by hydroxyl radical scavenger also proved the existence of ·OH radicals.[42,43] The above experiments indicated the presence of the ·OH during the interaction between GQDs and H_2O_2.[41−43] Like peroxidase mimics with iron centers,[43] it is known that electron transfer may occur between pairs of different oxidation states of GQDs to drive their catalytic activity.[44] The reaction mechanism could be deduced in Figure S3D (Supporting Information).

In view of excellent antibacterial capacity of ·OH and the high peroxidase-like activity of GQDs that could convert H_2O_2 into ·OH, the antibacterial system was designed. Herein, a disk diffusion assay and a growth-inhibition assay in liquid medium were used to evaluate the antibacterial capacity of the antibacterial systems (Figure 3 and Figure S4, Supporting Information).[45,46] The Gram-positive bacteria *E. coli* and Gram-negative bacteria *S. aureus* were used as models for the investigation of the antibacterial activities of the designed system. Log phase bacterial cells were used in all experiments. As shown in Figure 3, with the assistant of GQDs (100 μg/mL), H_2O_2 significantly decreased viabilities of both *E. coli* (Figure 3A) and *S. aureus* cells (Figure 3B) in a dose-dependent manner. Without addition of GQDs, just in the presence of a relative higher H_2O_2 concentrations (100 mM and 1 M H_2O_2 for *E. coli* and *S. aureus*, respectively), the survival rate of *E. coli* and *S. aureus* cells could be down to 10%. With the assistance of GQDs, the antibacterial ability of H_2O_2 had been remarkably improved; just 1 and 10 mM H_2O_2 could reach similar effect on *E. coli* and *S. aureus* cells, respectively. H_2O_2 exhibited different dose-dependent antibacterial effect on Gram-positive and Gram-negative bacteria, which could be due to different structures and chemical compositions of their cell walls and the "bacteria observer" effect.[45,47] Furthermore, without addition of H_2O_2, the GQDs did not show any antibacterial activity at the concentration range from 10 to 500 μg/mL for both *E. coli* and *S. aureus* cells, implying that the GQDs could serve as a catalyst to enhance the antibacterial activity of H_2O_2 in this system (Figure S5, Supporting Information). And as shown in Figure 3C,D, the enhanced antibacterial activity of H_2O_2 could also inhibit the growth of both *E. coli* (Figure 3C) and *S. aureus* bacteria (Figure 3D).[48,49] In addition, as shown in Figure S6 (Supporting Information), the GQD-based system also showed excellent antibacterial performance for *Staphylococcus epidermidis*, which was another kind of Gram-negative bacteria associated with infections.[50,51]

To investigate the changes of bacterial morphology induced by the antibacterial system, scanning electron microscope (SEM) was used to observe *E. coli* and *S. aureus* before and after GQDs/H_2O_2 treatment. As shown in Figure 4, untreated *E. coli* (Figure 4A) and *E. coli* cells treated just with GQDs (Figure 4C) were typically rod-shaped, both with smooth and intact cell walls, which also demonstrated that the GQDs showed little toxicity against bacteria. While, after treatment with H_2O_2 (Figure 4B) or with both GQDs and H_2O_2 (Figure 4D), the bacterial surface became rough and wrinkled since H_2O_2 and free radicals can oxidize the

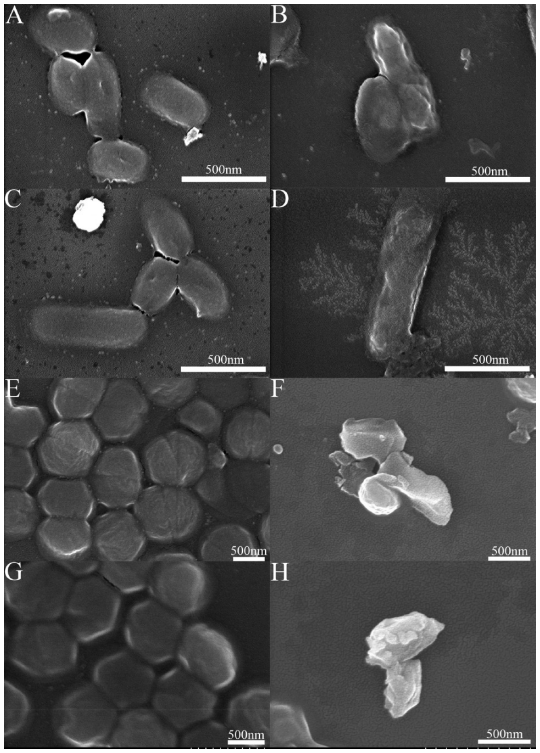

Figure 4. Typical SEM images of (A) *E. coli*; (B) *E. coli* treated with H_2O_2; (C) *E. coli* treated with GQDs; (D) *E. coli* treated with GQDs and H_2O_2; (E) *S. aureus*; (F) *S. aureus* treated with H_2O_2; (G) *S. aureus* treated with GQDs; (H) *S. aureus* treated with GQDs and H_2O_2.

lipid membrane and destroy the bacterial membranes.[52] As for *S. aureus* cells, the results of SEM experiments were similar to that of *E. coli* cells (Figure 4E–H). Without the addition of H_2O_2, the *S. aureus* cells were rod-shaped and smooth; in the presence of H_2O_2, *S. aureus* cells became rough and damaged. Moreover, according to typical transmission electron microscope (TEM) images, the GQDs adhered to the cell membrane of *E. coli* and *S. aureus* (Figure 5).[48,49,53] From the inhibition results (Figure 3 and Figure S4, Supporting Information), and TEM (Figure 5), we could conclude that the antibacterial activity of the system was not just a consequence of the bulk release of ·OH. GQDs, which adhered to the bacterial cell membrane, might catalyze the decomposition of H_2O_2 into ·OH on site and make the ·OH radicals damage the bacterial cell membrane more directly and effectively. In short, all these *in vitro* experiments indicated that our designed system had strong antibacterial properties against both Gram-positive and Gram-negative bacteria.

Biofilms on biomaterial implants are difficult to eradicate due to the protection offered by the biofilm mode of growth.[50] The effect of the GQD-based antibacterial system on the biofilm formation and destruction of the *S. aureus* was also explored. All the biofilm mass was quantified by crystal violet staining method.[54,55] In the experiments of biofilm destruction by GQD-based antibacterial system, treatment with both of GQDs

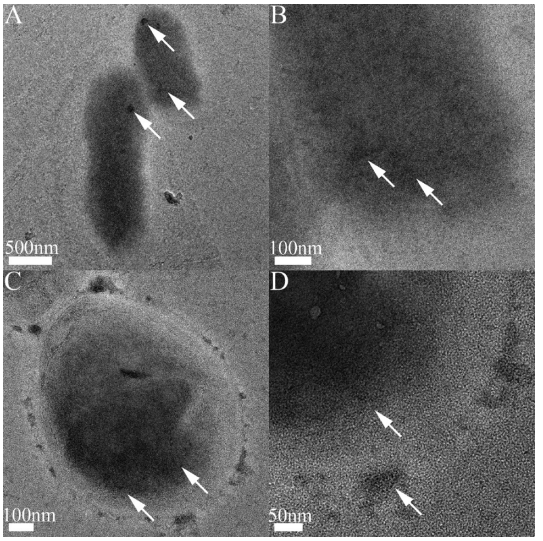

Figure 5. Internalization and location of GQDs in bacteria membrane. (A,B) Typical TEM images of *E. coli* with internalized GQDs. (C,D) Typical TEM images of *S. aureus* with internalized GQDs.

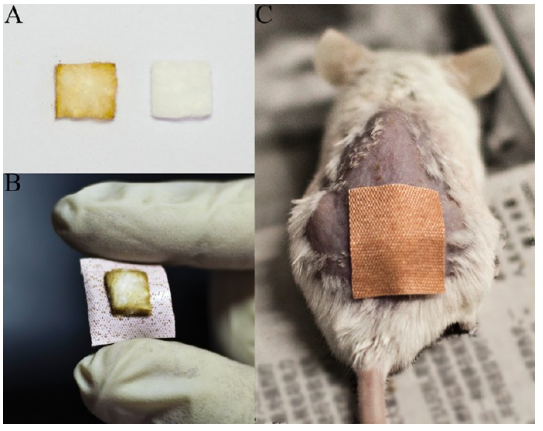

Figure 6. (A) The cotton fabric absorbed with (left) and without (right) GQDs. (B) The obtained GQD-Band-Aid. (C) The mouse treated with GQD-Band-Aid.

(100 μg/mL) and H_2O_2 (100 mM) for 12 h in biofilm minimal media (Tryptone Soy Broth medium) resulted in obvious reduction in remaining biofilms (Figure S7, Supporting Information). In contrast, similar to control wells treated with neither GQDs nor H_2O_2, wells treated with GQDs alone still showed clear biofilm bands. Even the treatment with just H_2O_2 (100 mM) displayed certain effect for biofilm destruction; the remaining biomasses were much larger than the wells treated with both of GQDs and H_2O_2. Moreover, as shown in Figure S8 (Supporting Information), when adding both GQDs (100 μg/mL) and H_2O_2 (1 mM) in biofilm minimal media, the biofilm formation of *S. aureus* was strongly inhibited, while similar to control group, when wells were treated with GQDs (100 μg/mL) or H_2O_2 (1 mM) alone, the clear biofilm bands could be observed. From the above results, GQDs could serve as a promoter to enhance the activity of H_2O_2 through converting H_2O_2 into ·OH for the

destruction and inhibiting formation of biofilm since the generated ·OH had a higher activity to oxidize nucleic acids, proteins and polysaccharides in the matrix of biofilm,[30] and the designed GQD-based antibacterial system could break down the existing biofilm and prevent formation of new biofilm as well.

Band-Aids are widely used in dressing the wound and avoiding disinfection.[56] The active ingredient in Band-Aids, benzalkonium chloride, has an excellent antibacterial activity but can lead to adverse drug reactions, such as allergic rhinitis, rhinitis medicamentosa, *etc*.[57−59] By taking advantage of the good biocompatibility of GQDs and their abilities to enhance H_2O_2 to kill bacteria, we designed a kind of Band-Aid, GQD-Band-Aid, and demonstrated its usage in wound disinfection to avoid bacterial infection (Figure 6).

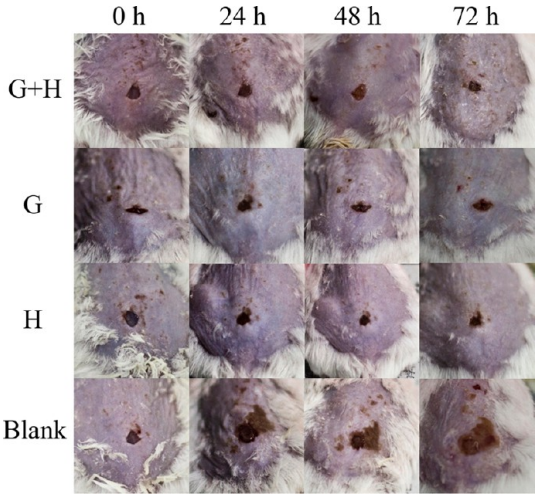

Figure 7. Photographs of wound on the mice from the four groups at different times during the therapeutic process. G+H: H_2O_2+GQD-Band-Aid group; G: GQD-Band-Aid group; H: H_2O_2+Blank-Band-Aid group; Blank: Saline+Blank-Band-Aid.

TABLE 1. Erythema and Oedema of Tested Mice Were Recorded[a]

	erythema					edema			
	G+H	G	H	Blank		G+H	G	H	Blank
24 h	−	−	−	+	24 h	−	+	+	+
48 h	−	−	−	+	48 h	−	+	+	+
72 h	−	−	−	+	72 h	−	+	+	+

[a] Each test article was tested three times on three mice. "−" no erytheme or edema. "+" with erytheme or edema. G+H: H_2O_2+GQD-Band-Aid group; G: GQD-Band-Aid group; H: H_2O_2+Blank-Band-Aid group; Blank: Saline+Blank-Band-Aid.

To assess the antibacterial efficacy of GQD-Band-Aid *in vivo*, we utilized Kunming mice with wound on their back as a model.[60] The mice were divided into four groups: treated with Saline+Blank-Band-Aid, GQD-Band-Aid, H_2O_2+Blank-Band-Aid, and H_2O_2+GQD-Band-Aid on their wounds, respectively. The concentration of H_2O_2 used in test therapy was 100 μM, which was much lower than that commonly used (0.5−3%, *ca*. 166 mM to 1 M) in wound disinfection. After injury on the back, photos were taken of the wounds of the mice from four different groups, and Band-Aids were changed at 24 h interval. During the therapeutic process, no change in body weight was observed, while the states of wounds were different. The wounds of mice that were treated with H_2O_2+GQD-Band-Aid did not appear to have any erythema and edema during the whole therapeutic process. After 72 h of therapy, the wounds of mice in this group formed scabs. The wounds of mice in other three groups appeared to have different levels of erythema and edema and did not form scabs (Figure 7 and Table 1). To define the host response to the infection, the tissues of wounds were harvested (Figure 8A), and the numbers of bacteria were quantified on each day of the therapeutic process (Figure 8B and Figure S9, Supporting Information). The bacteria from the tissues were cultured on agar plates overnight, and the grown colonies were counted for further analysis. The results demonstrated that the bacteria of H_2O_2+GQD-Band-Aids treated group were nearly four orders lower than that of saline treated group. In parallel, the GQD-Band-Aid and H_2O_2+Blank-Band-Aid groups also exhibited some antibacterial activity, but the bacteria of the two groups were one order lower than that of saline treated group, which implied that the combination of H_2O_2 and GQD-Band-Aids could kill bacteria during the

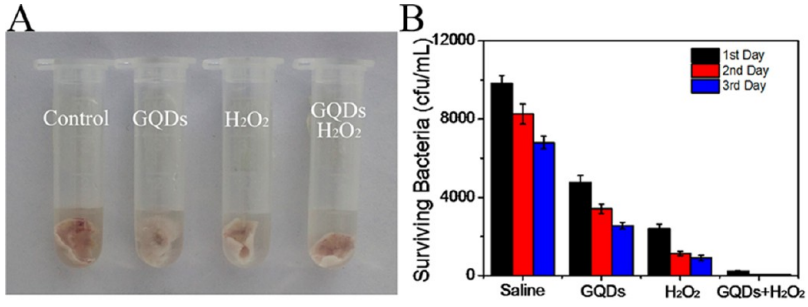

Figure 8. (A) The tissues of wound of the mice treated with Saline+Blank-Band-Aid, GQD-Band-Aid, H_2O_2+Blank-Band-Aid, and H_2O_2+GQD-Band-Aid once one day. (B) The surviving bacteria in the tissues of wound and colon were quantified. Error bars are taken from three mice per group.

wound antibacterial treatment most effectively. It was worth mentioning that even the GQDs did not display any antibacterial activity *in vitro*; the surviving bacterial of GQD-Band-Aid group were less than that of saline group, which might be attributed to that the injured cells could release H_2O_2, and the released H_2O_2 with the assistant of GQDs on the Band-Aid could kill bacteria on the wounds.[61−63]

CONCLUSIONS

In summary, an antibacterial system combining GQDs with low dose of common medical reagent, H_2O_2, was designed. The peroxidase-like activity originating from GQDs could catalyze H_2O_2 decomposition into ·OH. The conversion of H_2O_2 into ·OH improved the antibacterial performance of H_2O_2 since the ·OH had more potent antibacterial activity, which made it possible to avoid using high concentrations of H_2O_2 in wound disinfection. The designed system showed antibacterial properties against both Gram-negative (*E. coli*) and Gram-positive (*S. aureus*) bacteria *in vitro*. Moreover, to assess the antibacterial efficacy of the designed system for wound disinfection, the GQD-Band-Aids were prepared and showed excellent antibacterial property *in vivo* with the assistance of low concentration of H_2O_2. Our results indicate that GQD-Band-Aids have potential use for wound disinfection.

MATERIALS AND METHODS

Materials. Graphite was purchased from Sinopharm Chemical Reagent Co., Ltd. (Shanghai, China). Sulfuric acid, nitric acid, terephthalic acid and mannitol were purchased from Beijing Chemicals, Inc. (Beijing, China). 2,2′-Azinobis(3-ethylbenzthiazoline-6-sulfonate) (ABTS), sodium azide and crystal violet were obtained from Aladdin Chemistry Co., Ltd. (Shanghai, China). Luminol was purchased from Sigma-Aldrich. *E. coli* (ATCC 25922) and *S. aureus* (ATCC 25923) bacterial strains were obtained from Chuanxiang Biotechnology, Ltd. (Shanghai, China). *S. epidermidis* (ATCC 12228) bacterial strains were obtained from Fuxiang Biotechnology, Ltd. (Shanghai, China). Dialysis bags (molecular weight cut off = 1000 and 3500) were ordered from Shanghai Sangon Biotechnology Development Co., Ltd. Fabric and dressing were purchased from a drugstore. Ultrapure water was prepared using Milli-Q-Plus system water (18.2 MΩ cm) and used in all experiments. All reagents were used as received without any further purification.

Synthesis of GQDs. Graphene oxide (GO) was synthesized from graphite by a modified Hummers method.[64] The GQDs was prepared according to previous reports. Briefly, the GO solution (30 mL, 0.5 mg mL^{-1}) was first mixed with concentrated HNO_3 (8 mL) and H_2SO_4 (2 mL) carefully. Then, the mixture was heated and refluxed under microwave irradiation for 9 h in a WBFY-201 microwave oven equipped with an atmospheric reflux device (Gongyi Instrument Equipment Co., Ltd., China) operating at a power of 650 W. The product contained a brown transparent suspension and black precipitates. After cooling to room temperature, the mixture was placed under mild ultrasonication for few minutes, and the pH was tuned to 8 with Na_2CO_3 in an ice bath. The suspension was filtered through a 0.22 μm microporous membrane to remove the large tracts of GO, and a deep yellow solution (yield *ca.* 30%) was separated. The mixture was further dialyzed in a dialysis bag (retained molecular weight: 1000 Da), and greenish-yellow fluorescent GQDs were obtained.[35−37]

Bioassay. Kinetic measurements were carried out in time course mode by monitoring the absorbance change at 417 nm. Experiments were carried out using 75 μg mL^{-1} GQDs in a reaction volume of 500 μL buffer solution (25 mM Na_2HPO_4, pH 4.0, 37 °C) with 2.5 mM ABTS as substrate, and H_2O_2 concentration was 50 mM, unless otherwise stated. The Michaelis−Menten constant was calculated using the Lineweaver−Burk plot: $1/v = (K_m/V_{max})/C + 1/V_{max}$, where v is the initial velocity, V_{max} is the maximal reaction velocity, and C is the concentration of substrate.[20,38]

Apparatus and Characterization. UV absorbance measurements were carried out on a JASCO V-550 UV−vis spectrophotometer, equipped with a Peltier temperature control accessory. Fluorescence spectra were measured on a JASCO FP-6500 spectrofluorometer equipped with a temperature-controlled water bath. All spectra were recorded in a 1.0 cm path length cell. Chemiluminescence experiments were carried out on BPCL-2-TGC Ultra Weak Luminescence Analyzer. FT-IR characterization was carried out on a BRUKE Vertex 70 FT-IR spectrometer. The samples were thoroughly ground with exhaustively dried KBr. AFM measurements were performed using Nanoscope V multimode atomic force microscope (Veeco Instruments, USA). TEM images were recorded using a FEI TECNAI G^2 20 high-resolution transmission electron microscope operating at 200 kV. SEM images were recorded using a HITACHI S-4500 instrument. XPS measurement was performed on an ESCALAB-MKII spectrometer (VG Co., United Kingdom) with Al Kα X-ray radiation as the X-ray source for excitation. All the photos were taken by a Canon camera.

Bacterial Culture and Antibacterial Experiments. Monocolony of *E. coli*, *S. aureus* and *S. epidermidis* on the solid Luria−Bertani (LB) agar plate was transferred to 20 mL of liquid LB culture medium and grown at 37 °C for 12 h under 180 rpm rotation. Then the bacteria were diluted with broth to 10^6 cfu mL^{-1}.[45,46] The as-prepared bacteria solution (500 μL) was mixed with GQDs and H_2O_2 for 10 min. Then, the solution was placed on solid medium by spread plate method and cultured for 24 h before observing the number of the bacteria colonies. Control experiments were performed in parallel without H_2O_2 or GQDs.

Biofilm Formation of *S. aureus*. To develop biofilms, 10 μL of stationary growth phase *S. aureus* bacterial culture (requiring about 12 h growth at 37 °C in Tryptone Soy Broth (TSB) medium and the concentration of *S. aureus* cells: OD_{600nm} = 1.0) and 990 μL TSB medium (3%, containing 1% glucose) were into the 24-well microtiter plates. Microtiter plates were then incubated in air at 37 °C. The medium was discarded and freshly added every 24 h. After 48 h, each well was washed with PBS buffer under aseptic condition to eliminate medium and unbound bacteria.[65] The generated biofilms could be observed on the bottom of wells.

Biofilm Destruction of *S. aureus* by GQD-Based Antibacterial System. The obtained biofilms of *S. aureus* were treated with both GQDs (100 μg/mL) and H_2O_2 (100 mM), just H_2O_2 (100 mM) or GQDs (100 μg/mL) for 12 h in biofilm minimal media (TBS medium), respectively. The remaining biofilm was washed once with PBS (1.0 mL), before adding crystal violet stain (1.0 mL; 0.2% crystal violet, 1.9% ethanol and 0.08% ammonium oxalate in PBS). The plates were incubated on the bench for 20 min before washing the wells with PBS (2 × 1.0 mL). Photographs of the stained biofilms were obtained using a Canon digital camera. The amount of remaining crystal violet stained biofilm was quantified by adding 100% ethanol (1.0 mL) and measured OD_{590nm} of the homogenized suspension.[54,55] And the same 48 h old biofilms without any treatment in biofilm minimal media (TSB medium) for 12 h were measured as control groups.

Inhibiting Biofilm Formation of *S. aureus* by GQD-Based Antibacterial System. When developing biofilms of *S. aureus*, both GQDs (100 μg/mL) and H_2O_2 (1 mM), just H_2O_2 (1 mM) or GQDs (100 μg/mL) were added into TSB medium containing *S. aureus*

(Final concentration: OD_{600nm} = 0.01) in the 24-well microtiter plates, respectively. Microtiter plates were then incubated in air at 37 °C for 48 h. The generated biofilm was measured by crystal violet staining method as mentioned.[54,55] And the wells containing same concentration of *S. aureus* without adding GQDs or H_2O_2 in biofilm minimal media (TSB medium) for 48 h were measured as control groups.

Preparations of GQD-Band-Aid. According to the literature,[11] one square cotton fabric on the homemade negative pressure suction filter was mounted. GQDs solution (1.5 mg/mL) was added into the metal cylinder continuous until all GQDs solution passed through the cotton fabric. This filtration procedure was repeated until the solution was completely absorbed by cotton fabric. Then the square fabric disc was taken out and vacuum-dried at 60 °C. Resulting yellow samples were denoted as Fabric-GQDs. Then the Fabric-GQDs were fixed on the dressing purchased from drugstore, and the GQD-Band-Aids were obtained. The square cotton fabric of the same size without absorbed GQDs was fixed on the dressing, and the Blank-Band-Aids were obtained.

Mouse Injury Model. To evaluate the antibacterial effect of GQD-Band-Aid *in vivo*, the injury model was built. The four groups of 12 male Kunming mice with a *ca.* 4 mm^2 wound (6−8 weeks, 18−22 g, and three mice per group) were divided into Saline, GQDs, H_2O_2 and GQDs+H_2O_2 groups. The mice in four different groups with different Band-Aids on their wound were observed and photographed and Band-Aids were changed with 24 h interval. After 3 days, all mice were sacrificed, and the tissues of wounds were harvested, and the number of bacteria was quantified at each day of the therapeutic process. To determine the amount of bacteria in the tissues, wounds from four groups of mice were separated and homogenized in sterile saline. Aliquots of diluted homogenized intestinal tissues were placed on agar, on which the grown colonies were counted for analysis.[60] All animal procedures were in accord with the guidelines of the Institutional Animal Care and Use Committee.

Conflict of Interest: The authors declare no competing financial interest.

Acknowledgment. Financial support was provided by 973 project (2011CB936004, 2012CB720602) and NSFC (21210002, 91213302).

Supporting Information Available: Nine supplementary figures and a table. This material is available free of charge *via* the Internet at http://pubs.acs.org.

REFERENCES AND NOTES

1. Rizzello, L.; Pompa, P. P. Nanosilver-Based Antibacterial Drugs and Devices: Mechanisms, Methodological Drawbacks, and Guidelines. *Chem. Soc. Rev.* **2014**, *43*, 1501–1518.
2. Levy, S. B.; Marshall, B. Antibacterial Resistance Worldwide: Causes, Challenges and Responses. *Nat. Med.* **2004**, *10*, S122–S129.
3. Chernousova, S.; Epple, M. Silver as Antibacterial Agent: Ion, Nanoparticle, and Metal. *Angew. Chem., Int. Ed.* **2013**, *52*, 1636–1653.
4. Buffet-Bataillon, S.; Tattevin, P.; Bonnaure-Mallet, M.; Jolivet-Gougeon, A. Emergence of Resistance to Antibacterial Agents: The Role of Quaternary Ammonium Compounds—A Critical Review. *Int. J. Antimicrob. Agents* **2012**, *39*, 381–389.
5. Hajipour, M. J.; Fromm, K. M.; Akbar Ashkarran, A.; Jimenez de Aberasturi, D.; Larramendi, I. R. d.; Rojo, T.; Serpooshan, V.; Parak, W. J.; Mahmoudi, M. Antibacterial Properties of Nanoparticles. *Trends Biotechnol.* **2012**, *30*, 499–511.
6. Lee, J.; Mahendra, S.; Alvarez, P. J. J. Nanomaterials in the Construction Industry: A Review of Their Applications and Environmental Health and Safety Considerations. *ACS Nano* **2010**, *4*, 3580–3590.
7. Akhavan, O.; Ghaderi, E. Toxicity of Graphene and Graphene Oxide Nanowalls Against Bacteria. *ACS Nano* **2010**, *4*, 5731–5736.
8. Hu, W. B.; Peng, C.; Luo, W. J.; Lv, M.; Li, X. M.; Li, D.; Huang, Q.; Fan, C. H. Graphene-Based Antibacterial Paper. *ACS Nano* **2010**, *4*, 4317–4323.
9. Liu, S. B.; Zeng, T. H.; Hofmann, M.; Burcombe, E.; Wei, J.; Jiang, R. R.; Kong, J.; Chen, Y. Antibacterial Activity of Graphite, Graphite Oxide, Graphene Oxide, and Reduced Graphene Oxide: Membrane and Oxidative Stress. *ACS Nano* **2011**, *5*, 6971–6980.
10. Tu, Y. S.; Lv, M.; Xiu, P.; Huynh, T.; Zhang, M.; Castelli, M.; Liu, Z. R.; Huang, Q.; Fan, C. H.; Fang, H. P.; Zhou, R. H. Destructive Extraction of Phospholipids from *Escherichia coli* Membranes by Graphene Nanosheets. *Nat. Nanotechnol.* **2013**, *8*, 594–601.
11. Zhao, J.; Deng, B.; Lv, M.; Li, J.; Zhang, Y.; Jiang, H.; Peng, C.; Li, J.; Shi, J.; Huang, Q.; Fan, C. Graphene Oxide-Based Antibacterial Cotton Fabrics. *Adv. Healthcare Mater.* **2013**, *2*, 1259–1266.
12. Pinto, A. M.; Goncalves, I. C.; Magalhaes, F. D. Graphene-Based Materials Biocompatibility: A Review. *Colloids Surf., B* **2013**, *111*, 188–202.
13. Shen, J. H.; Zhu, Y. H.; Yang, X. L.; Li, C. Z. Graphene Quantum Dots: Emergent Nanolights for Bioimaging, Sensors, Catalysis and Photovoltaic Devices. *Chem. Commun.* **2012**, *48*, 3686–3699.
14. Zhang, Z. P.; Zhang, J.; Chen, N.; Qu, L. T. Graphene Quantum Dots: An Emerging Material for Energy-Related Applications and beyond. *Energy Environ. Sci.* **2012**, *5*, 8869–8890.
15. Zhu, S. J.; Tang, S. J.; Zhang, J. H.; Yang, B. Control the Size and Surface Chemistry of Graphene for the Rising Fluorescent Materials. *Chem. Commun.* **2012**, *48*, 4527–4539.
16. Li, L. L.; Wu, G. H.; Yang, G. H.; Peng, J.; Zhao, J. W.; Zhu, J. J. Focusing on Luminescent Graphene Quantum Dots: Current Status and Future Perspectives. *Nanoscale* **2013**, *5*, 4015–4039.
17. Sun, H.; Wu, L.; Wei, W.; Qu, X. Recent Advances in Graphene Quantum Dots for Sensing. *Mater. Today* **2013**, *16*, 433–442.
18. Wu, C.; Wang, C.; Han, T.; Zhou, X.; Guo, S.; Zhang, J. Insight into the Cellular Internalization and Cytotoxicity of Graphene Quantum Dots. *Adv. Healthcare Mater.* **2013**, *2*, 1613–1619.
19. Nurunnabi, M.; Khatun, Z.; Huh, K. M.; Park, S. Y.; Lee, D. Y.; Cho, K. J.; Lee, Y. K. *In Vivo* Biodistribution and Toxicology of Carboxylated Graphene Quantum Dots. *ACS Nano* **2013**, *7*, 6858–6867.
20. Zhang, Y.; Wu, C. Y.; Zhou, X. J.; Wu, X. C.; Yang, Y. Q.; Wu, H. X.; Guo, S. W.; Zhang, J. Y. Graphene Quantum Dots/Gold Electrode and Its Application in Living Cell H_2O_2 Detection. *Nanoscale* **2013**, *5*, 1816–1819.
21. Wu, X.; Tian, F.; Wang, W. X.; Chen, J.; Wu, M.; Zhao, J. X. Fabrication of Highly Fluorescent Graphene Quantum Dots Using L-Glutamic Acid for *In Vitro/In Vivo* Imaging and Sensing. *J. Mater. Chem. C* **2013**, *1*, 4676–4684.
22. Zheng, A. X.; Cong, Z. X.; Wang, J. R.; Li, J.; Yang, H. H.; Chen, G. N. Highly-Efficient Peroxidase-Like Catalytic Activity of Graphene Dots for Biosensing. *Biosens. Bioelectron.* **2013**, *49*, 519–524.
23. Vatansever, F.; de Melo, W. C. M. A.; Avci, P.; Vecchio, D.; Sadasivam, M.; Gupta, A.; Chandran, R.; Karimi, M.; Parizotto, N. A.; Yin, R.; Tegos, G. P.; Hamblin, M. R. Antimicrobial Strategies Centered around Reactive Oxygen Species—Bactericidal Antibiotics, Photodynamic Therapy, and beyond. *FEMS Microbiol. Rev.* **2013**, *37*, 955–989.
24. Schultke, E.; Hampl, J. A.; Jatzwauk, L.; Krex, D.; Schackert, G. an Easy and Safe Method to Store and Disinfect Explanted Skull Bone. *Acta Neurochir.* **1999**, *141*, 525–528.
25. Hayashi, E.; Mokudai, T.; Yamada, Y.; Nakamura, K.; Kanno, T.; Sasaki, K.; Niwano, Y. *In Vitro* and *In Vivo* Anti-*Staphylococcus aureus* Activities of a New Disinfection System Utilizing Photolysis of Hydrogen Peroxide. *J. Biosci. Bioeng.* **2012**, *114*, 193–197.
26. Loo, A. E. K.; Wong, Y. T.; Ho, R. J.; Wasser, M.; Du, T. H.; Ng, W. T.; Halliwell, B. Effects of Hydrogen Peroxide on Wound Healing in Mice in Relation to Oxidative Damage. *PLoS One* **2012**, *7*, e49215.

27. Finkel, T. Redox-Dependent Signal Transduction. *FEBS Lett.* **2000**, *476*, 52–54.
28. Apel, K.; Hirt, H. Reactive Oxygen Species: Metabolism, Oxidative Stress, And Signal Transduction. *Annu. Rev. Plant Biol.* **2004**, *55*, 373–399.
29. Natalio, F.; Andre, R.; Hartog, A. F.; Stoll, B.; Jochum, K. P.; Wever, R.; Tremel, W. Vanadium Pentoxide Nanoparticles Mimic Vanadium Haloperoxidases and Thwart Biofilm Formation. *Nat. Nanotechnol.* **2012**, *7*, 530–535.
30. Gao, L.; Giglio, K. M.; Nelson, J. L.; Sondermann, H.; Travis, A. J. Ferromagnetic Nanoparticles with Peroxidase-Like Activity Enhance the Cleavage of Biological Macromolecules for Biofilm Elimination. *Nanoscale* **2014**, *6*, 2588–2593.
31. Zychlinski, L.; Byczkowski, J. Z.; Kulkarni, A. P. Toxic Effects of Long-Term Intratracheal Administration of Vanadium Pentoxide in Rats. *Arch. Environ. Contam. Toxicol.* **1991**, *20*, 295–298.
32. Gonzalez-Villalva, A.; Fortoul, T. I.; Avila-Costa, M. R.; Pinon-Zarate, G.; Rodriguez-Lara, V.; Martinez-Levy, G.; Rojas-Lemus, M.; Bizarro-Nevarez, P.; Diaz-Bech, P.; Mussali-Galante, P.; Colin-Barenque, L. Thrombocytosis Induced in Mice after Subacute and Subchronic V_2O_5 Inhalation. *Toxicol. Ind. Health* **2006**, *22*, 113–116.
33. Ivankovic, S.; Music, S.; Gotic, M.; Ljubesic, N. Cytotoxicity of Nanosize V_2O_5 Particles to Selected Fibroblast and Tumor Cells. *Toxicol. In Vitro* **2006**, *20*, 286–294.
34. Worle-Knirsch, J. M.; Kern, K.; Schleh, C.; Adelhelm, C.; Feldmann, C.; Krug, H. F. Nanoparticulate Vanadium Oxide Potentiated Vanadium Toxicity in Human Lung Cells. *Environ. Sci. Technol.* **2007**, *41*, 331–336.
35. Li, L. L.; Ji, J.; Fei, R.; Wang, C. Z.; Lu, Q.; Zhang, J. R.; Jiang, L. P.; Zhu, J. J. A Facile Microwave Avenue to Electrochemiluminescent Two-Color Graphene Quantum Dots. *Adv. Funct. Mater.* **2012**, *22*, 2971–2979.
36. Sun, H. J.; Gao, N.; Wu, L.; Ren, J. S.; Wei, W. L.; Qu, X. G. Highly Photoluminescent Amino-Functionalized Graphene Quantum Dots Used for Sensing Copper Ions. *Chem.—Eur. J.* **2013**, *19*, 13362–13368.
37. Sun, H. J.; Wu, L.; Gao, N.; Ren, J. S.; Qu, X. G. Improvement of Photoluminescence of Graphene Quantum Dots with a Biocompatible Photochemical Reduction Pathway and Its Bioimaging Application. *ACS Appl. Mater. Interfaces* **2013**, *5*, 1174–1179.
38. Song, Y. J.; Qu, K. G.; Zhao, C.; Ren, J. S.; Qu, X. G. Graphene Oxide: Intrinsic Peroxidase Catalytic Activity and Its Application to Glucose Detection. *Adv. Mater.* **2010**, *22*, 2206–2010.
39. Lin, S. S.; Gurol, M. D. Catalytic Decomposition of Hydrogen Peroxide on Iron Oxide: Kinetics, Mechanism, and Implications. *Environ. Sci. Technol.* **1998**, *32*, 1417–1423.
40. Ishibashi, K.; Fujishima, A.; Watanabe, T.; Hashimoto, K. Detection of Active Oxidative Species in TiO_2 Photocatalysis Using the Fluorescence Technique. *Electrochem. Commun.* **2000**, *2*, 207–210.
41. Ge, S.; Liu, F.; Liu, W.; Yan, M.; Song, X.; Yu, J. Colorimetric Assay of K-562 Cells Based on Folic Acid-Conjugated Porous Bimetallic Pd@Au Nanoparticles for Point-of-Care Testing. *Chem. Commun.* **2014**, *50*, 475–477.
42. Li, Y. B.; Trush, M. A. DNA-Damage Resulting from the Oxidation of Hydroquinone by Copper Role for a Cu(II)/Cu(I) Redox Cycle and Reactive Oxygen Generation. *Carcinogenesis* **1993**, *14*, 1303–1311.
43. Xu, C.; Zhao, C.; Li, M.; Wu, L.; Ren, J.; Qu, X. Artificial Evolution of Graphene Oxide Chemzyme with Enantioselectivity and Near-Infrared Photothermal Effect for Cascade Biocatalysis Reactions. *Small* **2014**, *10*, 1841–1847.
44. Shinde, D. B.; Pillai, V. K. Electrochemical Resolution of Multiple Redox Events for Graphene Quantum Dots. *Angew. Chem., Int. Ed.* **2013**, *52*, 2482–2485.
45. Pu, F.; Liu, X.; Xu, B. L.; Ren, J. S.; Qu, X. G. Miniaturization of Metal-Biomolecule Frameworks Based on Stereoselective Self-Assembly and Potential Application in Water Treatment and as Antibacterial Agents. *Chem.—Eur. J.* **2012**, *18*, 4322–4328.
46. Ju, E. G.; Li, Z. H.; Li, M.; Dong, K.; Ren, J. S.; Qu, X. G. Functional Polypyrrole-Silica Composites As Photothermal Agents for Targeted Killing of Bacteria. *Chem. Commun.* **2013**, *49*, 9048–9050.
47. Ashkarran, A. A.; Ghavami, M.; Aghaverdi, H.; Stroeve, P.; Mahmoudi, M. Bacterial Effects and Protein Corona Evaluations: Crucial Ignored Factors in the Prediction of Bio-Efficacy of Various Forms of Silver Nanoparticles. *Chem. Res. Toxicol.* **2012**, *25*, 1231–1242.
48. Zhao, Y. Y.; Tian, Y.; Cui, Y.; Liu, W. W.; Ma, W. S.; Jiang, X. Y. Small Molecule-Capped Gold Nanoparticles as Potent Antibacterial Agents That Target Gram-Negative Bacteria. *J. Am. Chem. Soc.* **2010**, *132*, 12349–12356.
49. Zhao, Y.; Chen, Z.; Chen, Y.; Xu, J.; Li, J.; Jiang, X. Synergy of Non-antibiotic Drugs and Pyrimidinethiol on Gold Nanoparticles against Superbugs. *J. Am. Chem. Soc.* **2013**, *135*, 12940–12943.
50. Subbiandoss, G.; Sharifi, S.; Grijpma, D. W.; Laurent, S.; Van der Mei, H. C.; Mahmoudi, M.; Busscher, H. J. Magnetic Targeting of Surface-Modified Superparamagnetic Iron Oxide Nanoparticles Yields Antibacterial Efficacy against Biofilms of Gentamicin-Resistant *Staphylococci*. *Acta Biomater.* **2012**, *8*, 2047–2055.
51. Mahmoudi, M.; Serpooshan, V. Silver-Coated Engineered Magnetic Nanoparticles Are Promising for the Success in the Fight against Antibacterial Resistance Threat. *ACS Nano* **2012**, *6*, 2656–2664.
52. Imlay, J. A. Pathways of Oxidative Damage. *Annu. Rev. Microbiol.* **2003**, *57*, 395–418.
53. Durmus, N. G.; Taylor, E. N.; Kummer, K. M.; Webster, T. J. Enhanced Efficacy of Superparamagnetic Iron Oxide Nanoparticles Against Antibiotic-Resistant Biofilms in the Presence of Metabolites. *Adv. Mater.* **2013**, *25*, 5706–5713.
54. Barraud, N.; Kardak, B. G.; Yepuri, N. R.; Howlin, R. P.; Webb, J. S.; Faust, S. N.; Kjelleberg, S.; Rice, S. A.; Kelso, M. J. Cephalosporin-3′-diazeniumdiolates: Targeted NO-Donor Prodrugs for Dispersing Bacterial Biofilms. *Angew. Chem., Int. Ed.* **2012**, *51*, 9057–9060.
55. Peeters, E.; Nelis, H. J.; Coenye, T. Comparison of Multiple Methods for Quantification of Microbial Biofilms Grown in Microtiter Plates. *J. Microbiol. Methods* **2008**, *72*, 157–165.
56. Johnson & Johnson Consumer Companies, Inc. BAND-AID® Brand Adhesive Bandages Beginnings. http://www.band-aid.com/brand-heritage. 2014.
57. Graf, P.; Enerdal, J.; Hallen, H. Ten Days' Use of Oxymetazoline Nasal Spray with or without Benzalkonium Chloride in Patients with Vasomotor Rhinitis. *Arch. Otolaryngol.* **1999**, *125*, 1128–1132.
58. Marple, B.; Roland, P.; Benninger, M. Safety Review of Benzalkonium Chloride Used As a Preservative in Intranasal Solutions: An Overview of Conflicting Data and Opinions. *Otolaryngol.—Head Neck Surg.* **2004**, *130*, 131–141.
59. Graf, P. Rhinitis Medicamentosa. *Treat. Respir. Med.* **2005**, *4*, 21–29.
60. Li, L. L.; Wang, H. Antibacterial Agents: Enzyme-Coated Mesoporous Silica Nanoparticles as Efficient Antibacterial Agents *In Vivo*. *Adv. Healthcare Mater.* **2013**, *2*, 1298–1298.
61. Rieger, S.; Sagasti, A. Hydrogen Peroxide Promotes Injury-Induced Peripheral Sensory Axon Regeneration in the Zebrafish Skin. *PLoS Biol.* **2011**, *9*, e1000621.
62. Niethammer, P.; Grabher, C.; Look, A. T.; Mitchison, T. J. A Tissue-Scale Gradient of Hydrogen Peroxide Mediates Rapid Wound Detection in Zebrafish. *Nature* **2009**, *459*, 996–U123.
63. Moreira, S.; Stramer, B.; Evans, I.; Wood, W.; Martin, P. Prioritization of Competing Damage and Developmental Signals by Migrating Macrophages in the *Drosophila* Embryo. *Curr. Biol.* **2010**, *20*, 464–470.
64. Hummers, W. S.; Offeman, R. E. Preparation of Graphitic Oxide. *J. Am. Chem. Soc.* **1958**, *80*, 1339–1339.
65. Amorena, B.; Gracia, E.; Monzon, M.; Leiva, J.; Oteiza, C.; Perez, M.; Alabart, J. L.; Hernandez-Yago, J. Antibiotic Susceptibility Assay for *Staphylococcus aureus* in Biofilms Developed *In Vitro*. *J. Antimicrob. Chemother.* **1999**, *44*, 43–55.